International Journal of Sensors

Research Article
Published: 22 Jul, 2019

A Survey of SLAM Research based on LiDAR Sensors

Jingchao Yang[1], Yong Li[1,2], Lihao Cao[2], Yanmei Jiang[1], Liping Sun[1] and Qin Xie[1]*

[1]Hebei Jiaotong Vocational and Technical College, China

[2]College of Information Science and Engineering, Northeastern University, China

Abstract

With the wide application of Lidar sensors in many fields, the lidar-based SLAM technology has also developed rapidly. This paper first gives a brief overview of the application and practical significance of lidar-based SLAM technology in the fields of robotics, mapping and so on. Then, we introduce the commonly used experimental platform and data for lidar-based SLAM. According to the sensor and theoretical methods used in the classic SLAM technology scheme, the development history of SLAM technology and related algorithms are introduced. Finally, the discussion and prospects of lidar-based SLAM technology are discussed.

Keywords: SLAM; LiDAR; Survey; Sensor

Introduction

The field of robotics has always been a key area of research in industry and academia. Many robotic products have increased the productivity of human society and provided great convenience for human life. Robotic products require many theoretical and technical supports such as mechanical design, electronic design, environmental perception, positioning and mapping, decision making and control. Simultaneous Localization and Mapping (SLAM) is one of the research areas. It is the key to realizing the robot's autonomous movement [1]. The SLAM problem can be described as: placing a mobile robot in an unknown location in an unknown environment, whether the robot can incrementally construct a map of the surrounding environment while determining its position in the map [2]. The SLAM technology realizes positioning by acquiring surrounding scene information, and it constructs a map by using the result of the positioning, and it compares the obtained real-time environmental information with the map, and adjusts the previous positioning result and the current map, thereby completing the synchronous positioning and mapping task. It can be seen that positioning and mapping are two tasks that complement each other in SLAM technology.

At present, synchronous positioning and map construction technology are applied in many fields, such as unmanned delivery vehicles, auto-driving car local positioning, high-precision map construction, service robots, Automated Guided Vehicle (AGV), mobile measurement systems, indoor mapping Augmented Reality (AR) wearable devices and mobile AR, as shown in Figure 1, SLAM technology can provide real-time positioning and mapping functions for these applications. For example, the sweeping robot can clean the ground indoors, and obtain the surrounding environment information through its own sensors and determine its relative position and posture through SLAM technology. The environmental map, which combined with the positioning and mapping results to determine the cleaned area and the un-swept area, and that combined with the path planning function to achieve autonomous movement, and that ultimately achieve the function of autonomous, no-slip cleaning of the indoor ground.

The mobile measurement system of indoor is mainly used in the field of surveying and mapping. It usually uses multi-line LiDAR. It is hand-held or carried by the operator. It scans the indoor environment in real time. The SLAM technology is used to construct the indoor environment map in real time, and at the same time it locates its own position in the map. The mobile measurement system uses SLAM technology to obtain a point cloud map of the indoor environment. After that, the cloud map can be applied to some fields such as surveying and mapping, which greatly improves the efficiency of building indoor environment maps.

In outdoor environments, autonomous vehicles, unmanned delivery vehicles and drones can achieve high-precision positioning and mapping functions with high-precision GPS (Global Positioning System) equipment, but when GPS signals become weak or interrupted, for example, near the building, the positioning function may be temporarily disabled, and it needs to be positioned

OPEN ACCESS

Correspondence:
Yong Li, College of Information Science and Engineering, Northeastern University, Shenyang, 110819, China, E-mail: leoqiulin@126.com

Received Date: *29 May 2019*
Accepted Date: *17 Jul 2019*
Published Date: *22 Jul 2019*

Citation:
Yang J, Li Y, Cao L, Jiang Y, Sun L, Xie Q. A Survey of SLAM Research based on LiDAR Sensors. Int J Sens. 2019; 1(1): 1003.

by SLAM technology. Considering the cost, size, weight and ease of installation of the equipment, SLAM technology can bring great convenience to these applications. In closed environments, such as home environments, factory floors, tunnels, and mines, GPS signals are weak and can only be used to locate and map tasks with current sensor data. SLAM is the key technology to solve this problem.

Currently, the sensors used in the SLAM technology solution are mainly Light Detection and Ranging (LiDAR) and cameras. The cameras include monocular cameras, depth cameras and binocular cameras. Other auxiliary sensors include Inertial Measurement Units (IMUs), GPS devices, odometers, and the like. Emerging sensors include event cameras [3], solid-state LiDARs, and millimeter-wave LiDARs. The camera is severely affected by light and is limited in outdoor scenes. By transmitting and receiving the laser beam, the LiDAR uses the Time of Flight (ToF) method to obtain the distance of the scanning point from the center of the LiDAR, which is almost unaffected by the illumination conditions, and has a long detection range and high precision, in indoor and outdoor scenes. Both can be applied, but the disadvantage is that it is expensive.

At present, LiDAR mainly includes mechanical LiDAR, solid-state LiDAR and hybrid LiDAR. The most abundant output and application are mechanical LiDAR. This article uses mechanical LiDAR by default. The mechanical LiDAR fixes the laser transmitter and receiver on a rotating shaft, and rotates the fixed shaft through the motor while emitting the laser and receiving the laser to obtain point cloud data of the surrounding environment.

Mechanical LiDAR can be divided into single-line LiDAR and multi-line LiDAR according to the number of laser transmitters and receivers installed on the rotating shaft. The number of lines represents the number of pairs of laser transmitters and receivers. Single-line LiDAR are also called two-dimensional LiDAR, and multi-line LiDAR are also called three-dimensional LiDAR. The single-line LiDAR is fixed on a steering gear. The single-line LiDAR scans in the horizontal direction and rotates with the steering gear to obtain three-dimensional point cloud data in a certain field of view. Such a combined device is also considered as a three-dimensional LiDAR. These three mechanical LiDARs are shown in Figure 2. At present, multi-line LiDAR has been popularized. This article uses multi-line mechanical LiDAR by default.

Lidar obtains the distance of the scanning point from the center of the LiDAR by the time-of-flight method, so as to obtain the coordinates of the scanning point in the LiDAR coordinate system, which has the advantages of high frequency, high precision, long detection distance, and no influence of illumination, so the laser is based on the laser. LiDARs SLAM technology can be applied to large-scale, light-dark environments. However, the point cloud data obtained by LiDAR alone is used to estimate the pose. Since the initial value of the pose transformation is unknown in the iterative process, more iterations are needed, which affects the real-time performance of the SLAM algorithm. The current mainstream method is to use the IMU (Inertial Measurement Unit) sensor to provide a good initial value for the pose estimation process. The IMU includes three-axis accelerometers, three-axis gyroscopes, and magnetometers to capture the three-axis acceleration and triaxial angular velocity of motion in real time. Using these two kinds of data, the IMU and the mobile carrier pose can be solved to provide a good initial value for the pose estimation method.

Lidar and IMU-based SLAM technology is mainly used in the field of mobile robots and autonomous vehicles. Mobile robot positioning, path planning and navigation functions in simple scenes do not need to be positioned in three-dimensional space. Positioning and mapping in two-dimensional space can be considered, and cost considerations are considered. Mobile robot positioning and mapping in simple scenes mainly use single lines (2D) LiDAR. This SLAM technology scheme for positioning and mapping in a two-dimensional space is called a two-dimensional SLAM. For complex scenes, such as undulations on the ground and the need to go up and down stairs, robots need to use multi-line (3D) LiDAR to locate and construct 3D space maps in 3D space. Due to the uncertain roads, complicated road conditions and high safety requirements, autonomous vehicles need to be positioned and built in three-dimensional space. This SLAM technology for positioning and mapping in three dimensions is called a three-dimensional SLAM.

The 3D SLAM technology based on LiDAR is still in the stage of improving real-time, precision and robustness. There is no unified technical solution for the application of natural and varied real scenes. At the same time, there are point cloud sparseness and motion distortion and error. Accumulation, dynamic environmental impact, and long-running problems caused by large-scale environments still require new methods and even new sensors to improve the accuracy, real-time and robustness of SLAM technology. In terms of theory and application value, the three-dimensional SLAM technology based on LiDAR has important research significance.

Commonly used LiDAR SLAM Based Experimental Platform and Data

Velodyne 16-line LiDAR and point cloud data

The Velodyne 16 (VLP-16) line LiDAR is shown in Figure 3A and is produced by the company. It consists of 16 pairs of laser transmitters and receivers with a horizontal field of view of 360° and a vertical field of view of -15° to +15°. We call the point cloud obtained by a full-field scan of the LiDAR as a point cloud. The VLP-16 LiDAR uses the UDP protocol (User Datagram Protocol) to transmit point cloud data. The packet is a data unit, and a frame point cloud is composed of a plurality of packet combinations. The inherent parameters and operating parameters of the VLP-16 set by this algorithm are shown in Table 1.

In Table 1, the data transmission rate in the single return mode is 754 packet/s and the LiDAR speed is set to 10 Hz. Then, the LiDAR obtains 75.4 packets in one full field of view scan, that is, one frame of point cloud data is composed of 75.4 packets. For the convenience of calculation, in the single return working mode, 80 packets are used to form a frame point cloud.

The LiDAR uses the time-of-flight method to obtain the distance from the scanning point to the LiDAR center. The time-of-flight method means that the LiDAR transmitter emits an ultra-short laser pulse, and the laser is projected onto the object to diffusely reflect. The receiver of the LiDAR receives the diffuse reflection light, and calculates the scanning point according to the time when the laser beam is flying in the air. The distance from the LiDAR center is calculated as

$$d = c \times \Delta t / 2 \quad (1)$$

The distance from the scanning point to the center of the LiDAR is the speed of light, which is the time interval from the transmission to the reception of the laser.

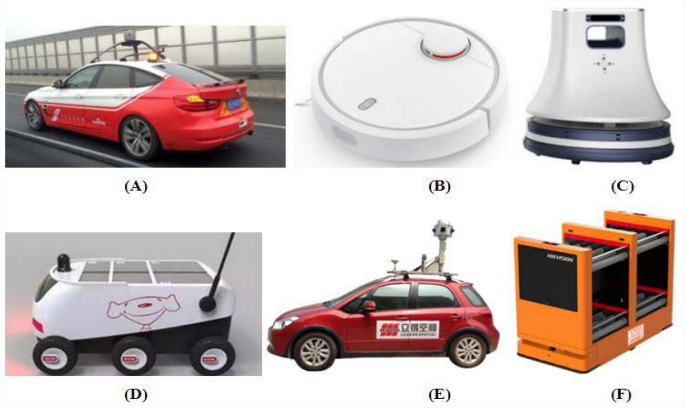

Figure 1: SLAM technology application. (A) Baidu unmanned vehicle; (B) Millet sweeping robot; (C) Think ZEUS service robot; (D) Unmanned delivery vehicle; (E) Space Mobile Measurement System; (F) Hikvision AGV car.

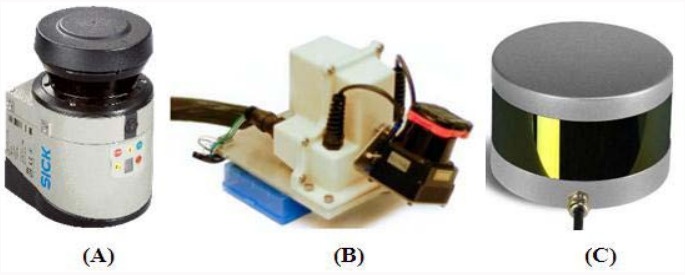

Figure 2: Mechanical LiDAR classifications. (A) SICK LMS111 Single line laser Lidar; (B) Single line laser Lidar and steering gear combination; (C) 16 Line lidar.

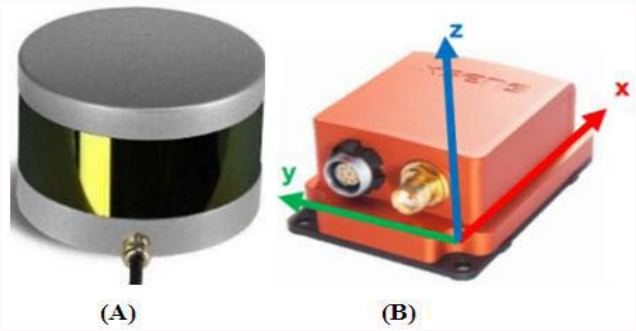

Figure 3: A Velodyne 16 LiDAR and an Xsens MTi-300 IMU, (A) Velodyne 16 Line Lidar; (B) Xsens MTi-300 IMU.

The vertical angle of each laser beam emitted by the LiDAR is fixed. After obtaining the distance between the scanning points and the center of the LiDAR, the coordinates of the point cloud are obtained by transforming the polar coordinates and Cartesian coordinates, and the point cloud coordinates are laser. The LiDAR coordinate system is the reference coordinate system. An example of point cloud data is shown in Figure 4.

Xsens MTi-300 IMU and IMU data

In the SLAM solution application, it is classified into the Inertial Measurement Unit (IMU) product class. It consists of a three-axis gyroscope, a three-axis accelerometer, and a magnetometer. It can output data such as triaxial angular velocity, three-axis acceleration and attitude in real time.

Figure 3B expresses the direction of the coordinate system of the IMU itself. The IMU sensor has determined the reference coordinate system of the measured three-axis angular velocity and attitude data at the time of production. The reference coordinate system of Xsens MTi-300 is Northeast Day. In the coordinate system, the positive direction of the X-axis points to the east, and the positive direction of the Y-axis points to the north, and the positive direction of the Z-axis points upward. It is the standard coordinate system applied in the field of aeronautical inertial navigation and geodesy.

The most important parameter of the IMU sensor is accuracy, and its accuracy affects the initial value of the point cloud registration, which affects the registration iteration time and registration error. The working parameters of MTi-300 are shown in Table 2.

Cartographer 3D data set

The Cartographer 3D dataset was opened by Google in 2016 and was acquired by a 3D backpacking system [4]. The system is equipped with two VLP-16 LiDARs and one IMU, as shown in Figure 5A, one LiDAR is placed horizontally and the other LiDAR is tilted. The acquisition scene is the Deutsche Science and Technology Museum in

Table 1: VLP-16 inherent parameters and working parameters.

Parameter Name	Numerical Value
Number of laser lines	16 lines
Precision	± 3 cm
Horizontal field of view	360°
Vertical field of view	-15° to +15°
Working frequency	10Hz
Detection distance	Up to 100 meters
Operating mode	Single return mode
Horizontal angular resolution	0.1° to 0.4°
Vertical angular resolution	2°
Data transfer rate	754 packets/second

Table 2: Xsens MTi-300 working parameters.

Parameter Name	Numerical Value
Working frequency	200Hz
Gyro bias stability	10°/h
Rolling angle accuracy	Static: 0.2°; dynamic: 0.3°
Pitch angle accuracy	Static: 0.2°; dynamic: 0.3°
Heading angle accuracy	1°

Munich, Germany. It provides a total of 25 pieces of data. Each piece of data contains two LiDAR data and IMU data. The LiDAR rotation frequency is 20 Hz. In the dual channel mode, the point cloud packet transmission rate is 1,508 packets/s and IMU data frequency is 250 Hz. But the data set does not provide real results for the trajectory.

Figure 5B shows the pose relationship between the sensors of the Cartographer backpack. The VR visualization package rviz is used. Two black cylinders represent the horizontal LiDAR and the tilt LiDAR. The orange cuboid is the IMU, and the red coordinate axes are all represented. The X axis and the green coordinate axis all represent the Y axis, and the blue coordinate axis represents the Z axis. The coordinate axis XYZ marked in the Figure 5B is the carrier coordinate system. The data set gives the pose matrix of the carrier coordinate system, and the two LiDAR coordinate systems and the IMU coordinate system for data coordinate conversion.

The university of Michigan north campus vision and LiDAR dataset

The University of Michigan North Campus Long-Term Vision and LiDAR Dataset, named NCLT dataset, collected by Carlevaris-Bianco [5] from January 2012 to April 2013 University of Michigan North Campus Collection. The mobile carrier uses a Segway robot, as shown in Figure 6A, with a panoramic camera Ladybug3, a Velodyne HDL-32E, a 32-line LiDAR, two Hokuyo single-line LiDARs, and a Microstrain 3DM-GX3, -45 model IMU. The speed of robot movement is between 1 m/s and 2 m/s. The coordinate system in the Figure 6 indicates the positional relationship between the carrier and the sensor coordinate system. Figure 6B and 6C are examples of outdoor and indoor scenes of the data set, respectively.

The Velodyne 32-line LiDAR has a horizontal field of view of 360°, a vertical field of view of +10.76° to -30.67°, a detection range of up to 70 m, and can transmit 1,803 packets in one second, and rotates at a frequency of 10 Hz during acquisition, so approximately 180 packets are composed, one frame of point cloud data. The GX3 IMU includes a three-axis accelerometer, gyroscope, magnetometer, etc., which

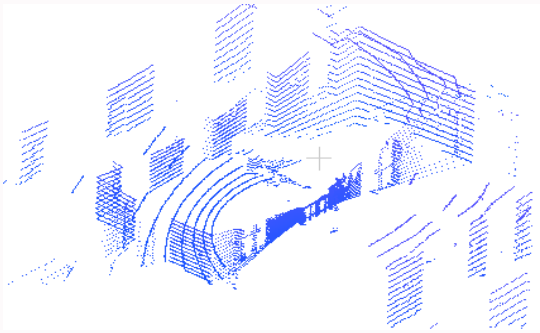

Figure 4: A frame of point cloud.

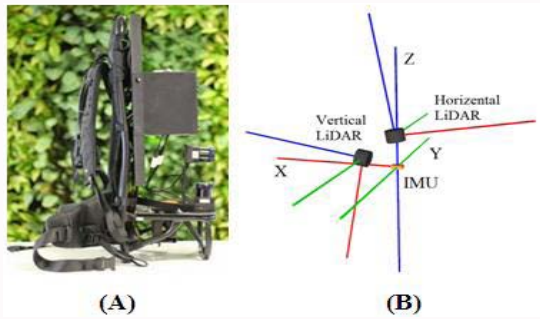

Figure 5: Cartographer backpack system and its coordinates, (A) Cartographer Backpack acquisition system; (B) Coordinate system representation.

can output speed, linear acceleration, angular velocity, attitude and other data. Unfortunately, the IMU has low accuracy. This algorithm uses only three-axis acceleration and three-axis angular velocity. The NCLT dataset provides accurate poses by combining RTK GPS equipment and SLAM algorithms, manually eliminating poor closed-loop constraints, and interpolating between poses using odometers, so trajectory accuracy can be verified based on this data set.

Research Status

The SLAM problem was first proposed in 1986. It refers to a mobile robot placed in an unknown location in an unknown environment, how to construct a globally consistent map of the surrounding scene and simultaneously determine its position and posture in the map. The development of SLAM technology is closely related to the development of sensors, probabilistic methods and nonlinear optimization methods. This section introduces the development of SLAM technology according to the evolution of sensors and theoretical methods used in the classic SLAM technology scheme. The development status of LiDAR-based SLAM technology at home and abroad is introduced in detail.

Probabilistic based SLAM scheme

In 2006 Bailey and Durrant-Whyte [6] summarized the development of SLAM technology from 1986 to 2006, mainly analyzing two SLAM technologies based on probabilistic methods: EKF-SLAM and Fast SLAM. In 1986, scholars began to apply probabilistic methods to robotics and artificial intelligence, and SLAM technology based on probabilistic methods continued to develop. After the publication of "State Estimation for Robotics" in 2016, the book details the process of expressing SLAM in three-dimensional space and the application of Lie algebra method in SLAM [7].

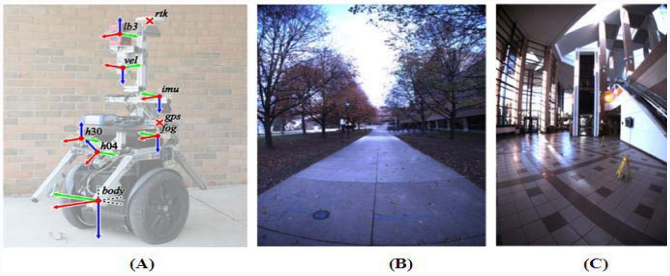

Figure 6: The NCLT dataset, (A) Acquisition platform; (B) Outdoor scene; (C) Indoor scene.

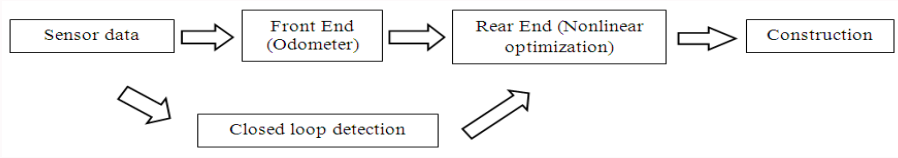

Figure 7: A classic SLAM frame based on nonlinear least squares.

Since 2007, representative SLAM schemes based on probabilistic methods have been proposed. Grisetti et al. [8] proposed an improved Rao-Blackwellized particle filter method, which reduced the number of sampled particles, and used single-line LiDAR to complete robot synchronization positioning and grid map construction. Kohlbrecher et al. [9] also used single-line LiDAR to propose a motion estimation method for scanning points and local raster map registration, and combined with 3D navigation equipment to complete 3D spatial synchronization positioning and raster map construction process. In a small-scale scenario, there is no need for closed-loop detection to achieve good accuracy. These two solutions are based on the SLAM classic solution for single-line LiDAR.

Davison et al. [10] first proposed the application of a probabilistic approach to a SLAM system using a monocular camera capable of tracking the three-dimensional pose of a monocular camera in an unknown environment. In the same year, Klein and Murray [11] proposed a SLAM system based on handheld cameras and applied to augmented reality. The SLAM framework for real-time positioning and mapping tasks using two parallel threads was proposed for the first time.

The probabilistic method needs to maintain a state matrix that grows with time, which brings computational efficiency problems. At the same time, it depends on the Markov assumption. There is no closed-loop detection link, and the cumulative error cannot be eliminated.

SLAM scheme based on nonlinear least squares

After 2012, scholars found that using the nonlinear least squares method to reduce the SLAM process error is sparse, the amount of calculation is acceptable, and the SLAM problem in the form of graphs is very intuitive. After that, many excellent visual SLAM schemes and three-dimensional LiDAR-based SLAM schemes were produced. The visual SLAM scheme includes the monocular camera schemes ORB-SLAM [12] and LSD-SLAM [13], the depth camera scheme [14] and the binocular camera scheme [15].

The classical framework of the SLAM method based on nonlinear least squares is shown in Figure 7. It consists of three links: the front end (also known as the odometer or tracking link), the back end (also known as the optimization link), and the closed-loop detection link (also known as the loop detection link). The odometer link estimates the position and attitude of the moving carrier when moving according to the real-time sensor data, mainly relies on the frame and frame or frame and sub-map registration method, and constructs the constraint between the frame and the frame or the frame and the sub-map from the registration result, thereby constructing a graph model. In the current technical solution, the current registration method is considered to achieve a registration between a frame and a frame or a frame and a sub-map, and the accuracy is acceptable, and there is a slight error, and the error may accumulate over time. The robustness of the registration method determines the robustness of the odometer and the entire SLAM system.

The most classic registration method is the Iterative Closest Point (ICP) algorithm [16]. The ICP method performs data association between two different point clouds by searching for the nearest point, usually using a k-dimensional tree. Organize point cloud data, accelerate search speed [17], and minimize the distance between two point clouds by nonlinear optimization method to solve the pose (position and attitude) transformation between two point clouds. The Generalized-ICP (GICP) [18] method combines the original ICP method with the point-to-surface ICP method, and proposes a planar to planar ICP method, which becomes the mainstream method in the ICP method variant.

Zhang and Singh [19] proposed a 3D LiDAR-based odometer scheme LOAM, which uses point-to-line, point-to-surface ICP algorithms to estimate inter-frame motion and pose transformation between frames and sub-maps. The scheme proposes a point cloud edge and plane point feature. The curvature threshold is used to extract edge points and plane points on each laser line of a frame point cloud. There is no descriptor, which is simple and effective. Use the k-D tree to organize the point cloud and complete the nearest neighbor search. Under the assumption of uniform motion for a short period of time, it is proposed that the inter-frame motion is estimated by the ICP method, and the point cloud motion distortion correction process is completed by the result.

Zhang et al. [20] proposed a real-time monocular visual odometer using depth information, a 3D LiDAR and a monocular camera to

map point clouds and images based on a uniform motion model and a calibrated pose transformation matrix. Not only the image feature matching point pairs with depth information are used, but also the feature matching point pairs without depth are used, and the constraint conditions at the time of registration are increased, which makes up for the problem that the available depth information of the image feature points caused by the point cloud sparseness is small, and the problem is improved. And the robustness of interframe motion estimation is improved.

Zhang et al. [21] combined the above two schemes to propose VLOAM. The inter-frame motion result obtained by the visual odometer is used as the initial value of the pose transformation of the LOAM system ICP algorithm. The whole system error accumulation is slow, which overcomes the rapid motion to some extent, the problem that caused the tracking to fail. The shortcoming is that the literature does not elaborate on the advantages and disadvantages of providing the initial value of the pose transformation based on the visual odometer and the initial value of the pose transformation based on the IMU [21].

Biber and Strasser [22] proposed using a normal distribution based NDT (Normal Distributions Transform), using a single-line LiDAR to divide a frame of point clouds obtained by the LiDAR into two-dimensional grids, assuming each grid. The points inside obey the normal distribution, the mean and covariance matrix of the point coordinates in each grid are counted, the normal distribution is used to represent the points in one grid, and the other frame point cloud is transformed by the initial pose transformation estimate. Within the grid, calculate the probability density value of the normal distribution at each point of the point, and use the sum of the density values corresponding to all points as the criterion for judging the registration result. The nonlinear optimization method is used to solve the pose transformation [23].

Magnusson et al. [24] proposed the NDT method applied to the 3D point cloud, the evaluation criteria are the same as the 2D NDT method, and summarizes the considerations of each link in the use of the NDT method. In 2012, Stoyanov et al. [25] first proposed that the point cloud or sub-map be described by a normal distribution model during the registration process. The registration process is to evaluate whether two normal distribution clusters are similar and estimate the pose transformation matrix. The process is called D2D-NDT (Distributions to Distributions Normal Distributions Transform). This method saves a lot of storage space by describing the frame or sub-map with a normal distribution.

Both literature [24] and literature [25] proposed D2D-NDT [26] and the mapping method NDT Fusion [27], which occupies grid map fusion. Both systems can be applied to large-scale dynamic environments, but there is no closed-loop detection.

Droeschel et al. [28] also used a raster map to express points in the grid in a normal distribution, the same as described above, and proposed to record the normal distribution in the grid as surfel (surface element). Because the Gaussian distribution probability density in the grid can express a spatial surface, it can be called a bin. Droeschel et al. [28] divided a grid map into multiple resolutions, with a high spatial resolution near the LiDAR and a low spatial grid resolution, which is consistent with LiDAR point cloud data because of the LiDAR horizontal angle resolution. The rate is fixed, so the farther the point cloud is from the LiDAR center, the more the data is occupied. The method of Gaussian distribution is less accurate when the number of points in the grid is small. The method is far from the LiDAR center. The range of the grid is relatively larger, which guarantees the number of points in the grid to a certain extent. Finally, the three-dimensional NDT registration method is used to achieve frame and sub-map registration. The program is applied to drones to track the rapid movement of drones. However, there is still no closed-loop detection link in this solution, and the cumulative error cannot be eliminated.

Later, Droeschel and Behnke [29] followed the above surfer-based registration method and combined the continuous-time expression trajectory estimation method to propose a new SLAM system. The system expresses the trajectory as a function related to continuous time [30,31]. The three-dimensional interpolation method is used to interpolate the pose, and the pose map is optimized hierarchically, which effectively improves the correction effect of the point cloud motion distortion, and theoretically can obtain the pose at any time. The scheme uses the pose optimization method to establish a closed loop detection link. The closed-loop detection link randomly selects candidate frames in the spatial range near the current point cloud pose, and uses the D2D-NDT method to register, and compares the similarity between the two sets of Gaussian distributions to determine whether closed loop constraints are detected.

In 2018, Behley and Stachniss [32] proposed a new SLAM scheme SuMa using 3D LiDAR. It also used a surfer-based map representation and solved the pose transformation matrix using the ICP method of frame and sub-map registration. The difference is that the scheme uses the OpenGL library for point cloud rendering processing. In the closed loop detection link, maps with different perspectives can be virtualized, so that even if there are only small overlapping regions of the point cloud and the map, the closed loop constraint can be detected and the closed loop can be improved; the robustness of the detection link.

Hess et al. [33] proposed a closed-loop detection method based on branch and bound algorithm, which searches for a point cloud and a sub-score in the pose space by taking a small discrete pose space near the current pose estimate. The map gets the best pose for a higher registration score. If it exists, the pose value is used as the initial value, and the new pose transformation is still estimated using the front-end registration method and used as the closed-loop constraint; if it does not exist, no closed loop is detected. The method is simple and effective, and is suitable for the real-time requirement of the SLAM algorithm. However, when the error accumulation exceeds the distance threshold, the closed-loop detection method will fail.

The closed-loop detection methods in the above laser SLAM scheme are all based on the geometric relationship. Currently in the visual SLAM scheme, the mainstream closed-loop detection method is the visual word bag model method [34]. Like the visual SLAM scheme, there is also a closed-loop detection method based on appearance in the laser SLAM scheme.

Steder et al. [35] combines the word bag model with the point cloud feature to detect closed loops in a 3D point cloud. Dube et al. [36] proposed a closed-loop detection method based on 3D point cloud object segmentation SegMatch, which combines the advantages of local features and global features of point clouds to enable reliable operation in large-scale, unstructured environments up to 1 Hz.

In 2018, Dube et al. [37] proposed the SegMap map representation

method and the positioning method based on incremental point cloud segmentation in the point cloud [38]. The SegMap method extracts point cloud features by means of descriptors created using machine learning methods, uses these feature points to construct a point cloud map and can add semantic information to the map; the segmentation-based incremental positioning method is based on point cloud maps. The positioning task provides a solution with an operating efficiency of up to 1 Hz, which overcomes the problem of large computational complexity of the registration method based on point cloud map to some extent.

In addition, Tan et al. [39] proposed a monocular SLAM system that is applied in a dynamic environment and has good robustness. In 2016, a monocular SLAM system based on robust keyframe mechanism was proposed and applied to the augmented reality field [40].

Then, Qin et al. [41] proposed a Visual-Inertial System (VINS), using a monocular camera and a low-cost IMU to estimate the carrier's 6-degree-of-freedom pose, and proposed the IMU data pre-integration method. A pre-integration result and feature points are combined to realize a high-precision visual-inertial odometry. A new closed-loop detection method is proposed to accomplish the low-computation relocation task.

Difficulties of Lidar-based SLAM

The point cloud data obtained by the multi-line mechanical LiDAR has a high horizontal angular resolution ranging from 0.1° to 0.4°. The rotation frequency can reach 10 Hz to 20 Hz. Take the Velodyne 16-line LiDAR as an example. It can scan about 120,000 three-dimensional points in one second, and the number of monocular image pixels with a height of 480 pixels and a width of 640 pixels large amount.

LiDAR is affected by physical devices. The angular resolution in the vertical direction is relatively low relative to the horizontal angle. At the same time, it is affected by the ranging principle. The farther away from the LiDAR center, the sparser the point cloud is, and when the distance is exceeded, the LiDAR does not receive. To the scanning point, the above three points make the point cloud obtained by the LiDAR sparse.

LiDAR transmits point cloud data through the UDP protocol and transmits it in units of packets. Several packets form a complete field of view scan. Taking the Velodyne 16-line LiDAR as an example, in the mode of returning the farthest distance point or the highest reflection intensity point, the transmission rate is 754 packets/s. When scanning at 10 Hz frequency, one frame point cloud (that is, complete one field of view). The point cloud obtained by the scan consists of 76 packages. The LiDAR acquires 76 packets while moving with the moving carrier, forming a frame point cloud. The three-dimensional points in such a frame point cloud are not in the same coordinate system, and are deformed compared with the point cloud obtained by the LiDAR static scanning once, that is, motion distortion is generated.

In summary, the LiDAR-based SLAM technology needs to overcome the problems of large computation, sparse point cloud and motion distortion. At the same time, SLAM technology generally has the following difficulties: balancing the real-time and precision relationship of the system, causing positioning failure due to rapid motion, dynamic object impact, and long-term operation caused by large-scale environment.

Acknowledgment

This research was funded by the Natural Science Young Foundation of Hebei Provincial, Department of Education QN2017324.

References

1. Cadena C, Carlone L, Carrillo H, Latif Y, Scaramuzza D, Neira J, et al. Past, Present, and Future of Simultaneous Localization and Mapping: Toward the Robust-Perception Age. IEEE Trans Robot. 2016;32(6):1309-32.
2. Durrant-whyte H, Bailey T. Simultaneous localization and mapping: part I. IEEE Robot Autom Mag. 2006;13(2):99-110.
3. Mueggler E, Rebecq H, Gallego G, Delbruck T, Scaramuzza D. The event-camera dataset and simulator: Event-based data for pose estimation, visual odometry, and SLAM. Int J Rob Res. 2017;36(2):142-9.
4. Jordan Novet. Google open-sources Cartographer 3D mapping library. Venture Beat. 2016 Oct 05.
5. Carlevaris-Bianco N, Ushani AK, Eustice RM. University of Michigan North Campus long-term vision and lidar dataset. Int J Rob Res. 2016;35(9)1023-35.
6. Bailey T, Durrant-Whyte H. Simultaneous localization and mapping (SLAM): part II. IEEE Robot Autom Mag. 2006;13(3):108-17.
7. Thrun S, Burgard W, Fox D. Probabilistic robotics. London: MIT Press; 2005.
8. Grisetti G, Stachniss C, Burgard W. Improved Techniques for Grid Mapping with Rao-Blackwellized Particle Filters. IEEE Trans Robot. 2007;23(1):34-46.
9. Kohlbrecher S, Stryk OV, Meyer J, Klingauf U. A flexible and scalable SLAM system with full 3D motion estimation. IEEE International Symposium on Safety, Security, and Rescue Robotics; 2011 Nov 1-5; Kyoto, Japan. New Jersey: IEEE; 2011.
10. Davison AJ, Reid ID, Molton ND, Stasse O. MonoSLAM: Real-Time Single Camera SLAM. IEEE Trans Pattern Anal Mach Intell. 2007;29(6):1052-67.
11. Klein G, Murray D. Parallel Tracking and Mapping for Small AR Workspaces. Int Symp Mix Augment Real. 2007:1-10.
12. Mur-Artal R, Montiel JMM, Tardos JD. ORB-SLAM: A Versatile and Accurate Monocular SLAM System. IEEE Trans Robot. 2015;31(5):1147-63.
13. Engel J, Schöps T, Cremers D. LSD-SLAM: Large-Scale Direct Monocular SLAM. In: Fleet D, Pajdla T, Schiele B, Tuytelaars T, editors. Computer Vision – ECCV 2014. Switzerland: Springer; 2014. p. 834-49.
14. Czupryński B, Strupczewski A. Real-time RGBD SLAM system. Society of Photo-optical Instrumentation Engineers Conference Series. International Society for Optics and Photonics. 2015:96622B.
15. Zhang G, Lee JH, Lim J, Suh IlH. Building a 3-D Line-Based Map Using a Stereo SLAM. IEEE Trans Robot. 2015;31(6):1364-77.
16. Besl PJ, Mckay ND. A method for registration of 3-D shapes. IEEE Trans Pattern Anal Mach Intell. 1992;14(2):239-56.
17. Pomerleau F, Colas F, Siegwart R. A Review of Point Cloud Registration Algorithms for Mobile Robotics. Now Foundations and Trends. 2015.
18. Segal A, Haehnel D, Thrun S. Generalized-ICP. Proceedings of Robotics Science and Systems. 2009 June 28-July 1; Seattle, USA. 2009.
19. Zhang J, Singh S. LOAM: Lidar Odometry and Mapping in Real-time. Proceedings of Robotics Science and Systems Conference. 2014.
20. Zhang J, Kaess M, Singh S. Real-time depth enhanced monocular odometry. International Conference on Intelligent Robots and Systems (IROS); 2014 September 14-18; Chicago, IL, USA. New Jersey: IEEE/RSJ;

2014. p. 4973-80.

21. Zhang J, Singh S. Visual-lidar odometry and mapping: low-drift, robust, and fast. International Conference on Robotics and Automation (ICRA); 2015 May 26-30; Seattle, Washington, USA. New Jersey: IEEE; 2015. p. 2174-81.

22. Biber P, Strasser W. The normal distributions transform: a new approach to laser scan matching. Proceedings of IEEE/RSJ International Conference on Intelligent Robots and Systems (IROS); 2003 Oct 27-31; Las Vegas, NV, USA. New Jersey: IEEE; 2003. p. 2743-8.

23. Richard W. CottleMukund N. Thapa. Linear and Nonlinear Optimization. Part of the International Series in Operations Research & Management Science book series (ISOR, volume 253).

24. Magnusson M, Lilienthal A, Duckett T. Scan registration for autonomous mining vehicles using 3D-NDT. J Field Rob. 2007;24(10):803-27.

25. Stoyanov T, Magnusson M, Andreasson H, Lilienthal AJ. Fast and accurate scan registration through minimization of the distance between compact 3D NDT representations. Int J Rob Res. 2012;31(12):1377-93.

26. Stoyanov T, Saarinen J, Andreasson H, Lilienthal AJ. Normal Distributions Transform Occupancy Map fusion: Simultaneous mapping and tracking in large scale dynamic environments. IEEE/RSJ International Conference on Intelligent Robots and Systems; 2013 Nov 3-7; Tokyo, Japan. New Jersey: IEEE; 2013. p. 4702-8.

27. Saarinen J, Andreasson H, Stoyanov T, Ala-Luhtala J, Lilienthal AJ. Normal Distributions Transform Occupancy Maps: Application to large-scale online 3D mapping. IEEE International Conference on Robotics and Automation; 2013 May 6-10; Karlsruhe, Germany. New Jersey: IEEE; 2013. p. 2233-8.

28. Droeschel D, Stuckler J, Behnke S. Local multi-resolution representation for 6D motion estimation and mapping with a continuously rotating 3D laser scanner. IEEE International Conference on Robotics and Automation (ICRA); 2014 May 31- June 7; Hong Kong, China. New Jersey: IEEE; 2014. p. 5221-6.

29. Droeschel D, Behnke S. Efficient Continuous-time SLAM for 3D Lidar-based Online Mapping. IEEE International Conference on Robotics and Automation (ICRA); 2018 May 21-25: Brisbane, QLD, Australia. New Jersey: IEEE; 2018. p. 1-9.

30. Lovegrove S, Patron-Perez A, Sibley G. Spline Fusion: A continuous-time representation for visual-inertial fusion with application to rolling shutter cameras. In: Burghardt T, Damen D, Mayol-Cuevas W, Mirmehdi M, editors. Proceedings of the British Machine Vision Conference; 2013 Sept 9-13; Bristol, UK. Bristol: BMVA; 2013. p. 93.1-93.12.

31. Park C, Moghadam P, Kim S, Elfes A, Fookes C, Sridharan S. Elastic LiDAR Fusion: Dense Map-Centric Continuous-Time SLAM. IEEE International Conference on Robotics and Automation (ICRA); 2018 May 21-25; Brisbane, QLD, Australia. New Jersey: IEEE; 2018. p. 1206-13.

32. Behley J, Stachniss C. Efficient Surfel-Based SLAM using 3D Laser Range Data in Urban Environments. In: Kress-Gazit H, Srinivasa S, Howard T, Atanasov N, editors. Proceedings on Robotics: Science and Systems XIV; 2018 June 26- 30; Pennsylvania, USA; 2018.

33. Hess W, Kohler D, Rapp H, Andor D. Real-time loop closure in 2D LIDAR SLAM. IEEE International Conference on Robotics and Automation (ICRA); 2016 May 16-21; Stockholm, Sweden. New Jersey: IEEE; 2016. p. 1271-8.

34. Galvez-Lopez D, Tardos JD. Bags of Binary Words for Fast Place Recognition in Image Sequences. IEEE Trans Robot. 2012;28(5):1188-97.

35. Steder B, Ruhnke M, Grzonka S, Burgard W. Place recognition in 3D scans using a combination of bag of words and point feature based relative pose estimation. IEEE/RSJ International Conference on Intelligent Robots and Systems, IROS; 2011 Sept 25-30; San Francisco, CA, USA. New Jersey: IEEE; 2011. p. 1249-55.

36. Dube R, Dugas D, Stumm E, Nieto J, Siegwart R, Cadena C. SegMatch: Segment based loop-closure for 3D point clouds. arXiv: Robotics. 2016;19(7):890-905.

37. Dube R, Cramariuc A, Dugas D, Nieto J, Siegwart R, Cadena C. SegMap: 3D Segment Mapping using Data-Driven Descriptors. In: Kress-Gazit H, Srinivasa S, Howard T, Atanasov N, editors. Robotics Science and Systems Online Proceedings, XIV; 2018 June 26-30; Pittsburgh, PA, USA; 2018.

38. Dube R, Gollub M, Sommer H, Igilitschenski I, Siegwart R, Cadena C, et al. Incremental-segment-based localization in 3-D point clouds. IEEE Robot Autom Lett. 2018;3(3):1832-9.

39. Tan W, Liu H, Dong Z, Zhang G, Bao H. Robust monocular SLAM in dynamic environments. IEEE International Symposium on Mixed and Augmented Reality (ISMAR); 2013 Oct 1-4; Adelaide, SA, Australia. New Jersey: IEEE; 2013. p. 209-18.

40. Liu H, Zhang G, Bao H. Robust Keyframe-based Monocular SLAM for Augmented Reality. IEEE International Symposium on Mixed and Augmented Reality (ISMAR); 2016 Sept 19-23; Merida, Mexico. New Jersey: IEEE; 2016. p. 1-10.

41. Qin T, Li P, Shen S. VINS-Mono: A Robust and Versatile Monocular Visual-Inertial State Estimator. IEEE Trans Robot. 2018;34(4):1004-20.